Suppression of a structural phase transition by an orientational disorder of counter anions in an organic conductor, β´´-β´´-$(BEDT\text{-}TTF)_2ClC_2H_4SO_3$

Hiroki Akutsu,[†,*] *Mikio Uruichi*,[‡] *Shusaku Imajo*,[§] *Koichi Kindo*,[§] *Takato Masuta*,[†] *Haruhito Manabe*,[†] *Yasuhiro Nakazawa*,[†] *and Scott S. Turner*[¶]

[†]Department of Chemistry, Graduate School of Science, Osaka University, 1-1, Machikaneyama, Toyonaka, Osaka 560-0043, Japan.

[‡]Institute for Molecular Science, Okazaki, Aichi 444-8585, Japan.

[§] Institute for Solid State Physics, The University of Tokyo, Kashiwa 277-8581, Japan.

[¶]School of Chemistry and Chemical Engineering, University of Surrey, Guildford, Surrey, GU2 7XH, U.K.

Keywords: Organic Conductors, Structural Phase Transition, Polar, Dope, BEDT-TTF

Abstract

In 2022 we reported that the β´´-(BEDT-TTF)$_2$ClC$_2$H$_4$SO$_3$ salt (**1**) has a phase transition at 210 K on cooling and 260 K on heating, which was suggested as a non-doped-to-doped transition. During the synthesis of **1**, a second salt was co-produced, the structure and properties of which are reported here. The new salt, β´´-β´´-(BEDT-TTF)$_2$ClC$_2$H$_4$SO$_3$ (**2**) has the same composition and is isomorphous to **1L**, the low temperature phase of **1**. However, the salt shows no phase transition. **1H**, the high temperature phase of **1**, displays rotational disorders of the -SO_3^- groups. In contrast the anions in **2** have no rotational disorders but have orientational disorder. Approximately 13 % of the anions in **2** have their orientation opposed the remaining anions. The geometrically calculated shortest O···O distance is 2.24 Å if neighbour -SO_3^- groups are able to rotate freely. This is 1.1 Å shorter than the sum of the van der Waals radii, and therefore this is too close to allow free rotation. Therefore, it is proposed that **2** has no rotational disorder which leads to no phase transition as is observed in **1**.

Introduction

Over the past half century of research into molecule-based organic conductors the most widely used component molecule is BEDT-TTF (bis(ethylenedithio)tetrathiafulvalene). For example, a range of 2:1 salts of BEDT-TTF with counter anions, (BEDT-TTF)$_2$X (X is a monoanion), show a wide variety of physical properties. These appear as insulating, semiconducting, metallic, superconducting, dia-, para-, antiferro-, or ferro-magnetic, and so on. In spite of the fact that each conducting layer consists of the same cationic BEDT-TTF molecule with the formula charge of +0.5, the physical properties of the salts are dependent on the donor arrangements (α-, β-, β´´-, δ-, δ´-, κ-, λ-, etc.) and the shape and size of the interleaved counter anions.[1] We have also suggested

for more than ten years that the dipole moment of the counterion layer has a significant effect on the electronic structure of the donor layer.[2-11]

We previously reported two BEDT-TTF salts with the $ClC_2H_4SO_3^-$ anion.[11,12] The first example is δ-(BEDT-TTF)$_2$$ClC_2H_4SO_3$·$H_2O$, which shows a structural phase transition at around 160 K, below which the donor arrangement changes to a δ´-type. A further transition occurs below 140 K, when localized electrons on the donor layers show spin ladder behavior.[12] The second example is β´´-(BEDT-TTF)$_2$$ClC_2H_4SO_3$ (**1**),[11] which shows a phase transition at 210 or 260 K upon decreasing or increasing the temperature, respectively. The anionic layers of the high temperature phase (**1H**) has no component of dipole moment perpendicular to the donor layer. On the other hand, the anionic layers of the low temperature phase (**1L**) have a small but significant component of dipole moment normal to the donor layers. **1L** has two crystallographically independent donor layers, A and B, each of which is bordered by the positive or negative side of the anionic layer's dipole (←B→A←B→A←). The different cation-anion interactions lead to A and B layers with different oxidation states. Therefore, we termed the transition a temperature-induced non-doped-to-doped transition.

Here we report the third polymorph, β´´- β´´-(BEDT-TTF)$_2$$ClC_2H_4SO_3$ (**2**), which is isomorphous to **1L** with the same chemical composition. However, **2** does not show the same phase transition as **1** and maintains two crystallographically independent donor layers at least up to room temperature. **2** has disorder in its anionic layer, where *ca*. 13 % of $ClC_2H_4SO_3^-$ are orientated in the opposite direction to the remaining anions ($^-O_3SC_2H_4Cl$). The structure, physical properties and the effect of the disorder of **2** are discussed.

Experimental

Salt **2** was prepared using the same procedure as reported previously for salt **1**.[11] Both **1** and **2** co-existed in the same sample batch, and were separated using a sharpened tooth pick under a microscope. The X-ray diffraction measurements at 100 and 290 K were performed on a Rigaku XtaLAB Synergy Custom with MicroMax-007 HF/VariMax rotating-anode X-ray generator with confocal mono-chromated MoKα radiation. AC electrical resistivity measurements from 4.2 K to room temperature were performed by the conventional four-probe method using a HUSO HECS 994C1 four channel resistivity meter with cooling and heating rates of ≈ 0.5 K/min. Magnetic susceptibility of a polycrystalline sample was measured at 3000 G in the range of 2-300 K using a Quantum Design MPMS-2S SQUID magnetometer. The data were corrected for a contribution from the aluminum foil sample holder. The diamagnetic contribution of the sample was estimated from Pascal's constants, which were subtracted from the data. Dipole moments of the anions were calculated by MOPAC2016[13] with PM3 Hamiltonian on Winmostar V9.2.5, using the molecular geometries from the crystal structures with no further structure optimization. Effective voltages caused by the dipole moment of the anion layers were estimated following Suda *et al*.[14] Band structures were calculated using a tight binding calculation package based on extended Hückel theory written by Prof. Takehiko Mori.[15] Raman spectra were measured on a Renishaw Ramascope, in Via Reflex. A diode laser (785 nm) was used to excite the sample, focused on an area of diameter ca. 5 μm, with ~0.1 mW power. The single crystal was fixed with silicon grease on a copper sample holder. The incident light was polarized to *c* and *b* axes for **2**, respectively. A low temperature spectrum was measured using a helium-flow cryostat Oxford MicrostatHe. Magnetoresistance measurements were performed in a ^{4}He-cryostat with a non-destructive 60 T pulse magnet with a 36 ms duration of the pulsed magnetic fields.

Results and discussion

1L and **2** are isomorphous and have the same composition, but the crystal appearances are very different, as shown in Figure 1. Therefore, these crystals are easily separated by hand. Table 1 shows X-ray crystallographic data of both **1** and **2** at 100 and 290 K.

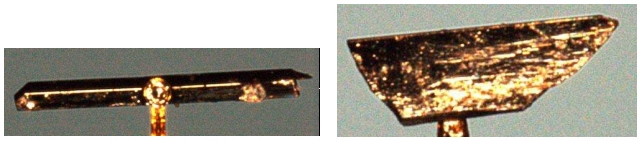

(a) (b)

Figure 1. Crystals of (a) **1** and (b) **2** used for X-ray analysis.

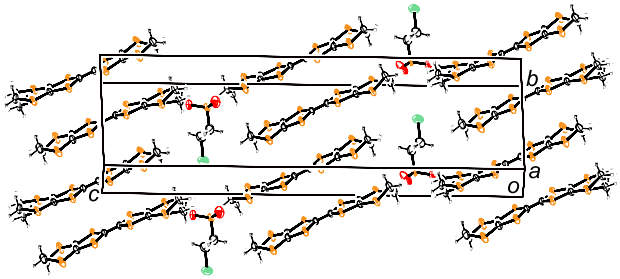

(a)

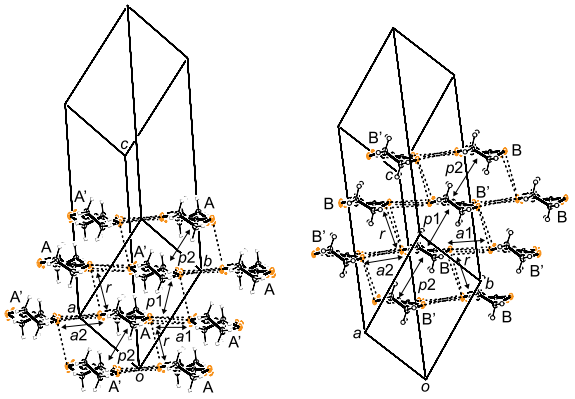

(b)

Figure 2. (a) Crystal structure of **2** at 290 K, where only the major fraction of anions with occupancy of 0.846(2) are shown and the disordered minor fraction with occupancy of 0.154(2) are omitted. (b) Donor arrangements of the A layer (left) and B layer (right) at 100 K.

Table 1. X-ray crystallographic data of **1** and **2** at 100 and 290 K.

	1H	**1L**	**2**	**2**
Composition		$(BEDT\text{-}TTF)_2ClC_2H_4SO_3$		
T / K	290	100	290	100
Space group	$P2_1/m$	$P\bar{1}$	$P\bar{1}$	$P\bar{1}$
a / Å	5.8446(4)	5.77900(10)	5.87215(13)	5.79124(19)
b / Å	33.2755(19)	8.7395(2)	8.81591(14)	8.7438(2)
c / Å	8.8244(6)	33.1806(10)	33.3511(7)	33.2059(10)
α / °	90.0	88.953(2)	88.3780(15)	89.027(2)
β / °	102.911(7)	86.170(2)	85.5678(18)	86.094(3)
γ / °	90.0	76.872(2)	76.3077(16)	76.761(3)
V / Å^3	1672.80(19)	1628.35(7)	1672.36(6)	1632.97(9)
Z	2	2	2	2
R	0.047	0.085	0.050	0.054
wR	0.121	0.211	0.136	0.157

CCDC numbers of **2** at 290, 250, 200, 150 and 100 K are 2365080, 2365159, 2365160, 2365087 and 2365089, respectively.

Figure 2a and 2b show the crystal structure of **2** at 290 K and its donor arrangement at 100 K. The anion of **2** is disordered as shown in Figure 3. At 100 K, approximately 13 % of anions are directed in opposition to the remaining 87 %.[16] In other words, 87 % of $^{-}O_3SC_2H_4Cl$ and 13 % of $ClC_2H_4SO_3^{-}$ are superimposed. The doping ratio is different from that of **1L** due to the disorder. The presence of 13 % of anions rotated by 180°reduces the anion layer's dipole moment by about 34 %. The dipole moments of the major (≈ 87 %) and minor (≈ 13 %) anion fractions were calculated using MOPAC2016/PM3 to be 6.98 and 6.74 debye, respectively. The angles between the dipole moment vectors of the major and minor anion fractions and the donor layer are 7 and -7°, respectively. Using these values and an equation by Suda *et al.*,[14] the effect of the anionic layer's dipole moment on the adjacent donor layer is calculated, to be 0.32 eV for the major

fraction and 0.31 eV for minor fraction. Taking account of their occupancies and opposite orientations, the effective voltage E_e of the anion layer of **2** is as follows.

$$E_e = 0.32 \text{ eV} \times 0.87 - 0.31 \text{ eV} \times 0.13 = 0.24 \text{ eV} \qquad (1)$$

The difference in charge (Q) between the donor layers A and B can be roughly estimated using the calibration curve between Q and E_e,[11] which is ≈ 0.01: the charges associated with layer A and B are suggested to be 0.495 and 0.505, respectively.

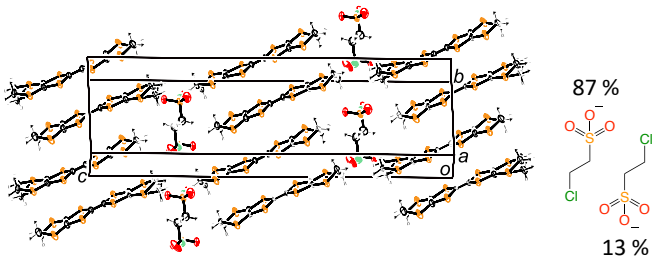

Figure 3. Crystal structure of **2** at 100 K, where disordered anions are shown.

The temperature dependence of electrical resistivity of **2** is shown in Figure 4. Metallic behaviour is observed from room temperature to approximately 80 K, below which there is a gradual increase of resistivity. The relatively low resistivity at temperatures below the metal-insulator transition seems to be caused by the doping effect, despite a doping level that is approximately half of **1L**. A hysteresis in the resistivity measurement is observed, suggesting that a very broad phase transitions starts at 250 K and ends at 50 K. However, the resistivity curve has no discontinuities similar to those observed at 210 and 260 K for **1**, again indicating that only **1L** shows a structural phase transition.

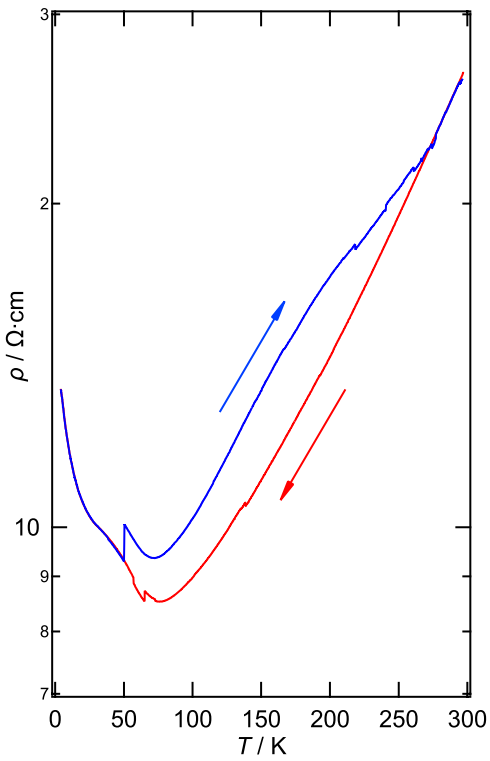

Figure 4. Temperature-dependent electrical resistivity of **2**.

The temperature-dependent magnetic susceptibility of **2** is shown in Figure 5 and has similar behaviour to that of **1**. However, the magnetic susceptibility curve of **1** has small anomalies at 210 (cooling) and 260 K (heating), corresponding to its resistivity jumps. On the other hand **2** has small anomalies at 250 K for both the cooling and heating curves. Other small anomalies are observed at the T_{MI} (metal-insulator transition temperature), below which magnetic susceptibility decreases more rapidly to become $\approx 1 \times 10^{-4}$ emu/mol. This support the suggestion that the ground state is not metallic and has only a small number of charge carriers although the resistivity increase below T_{MI} by less than 40 % is quite small. In addition, there seems to be another anomaly in the magnetic data at 290 K. The charge difference between the A and B layers of compound **2** is half of that of **1** but both magnetic behaviours are quite similar,

suggesting that the doping effect is not expressed in the magnetic data. This is expected because the number of doping carriers (≈ 0.1 %) is small.

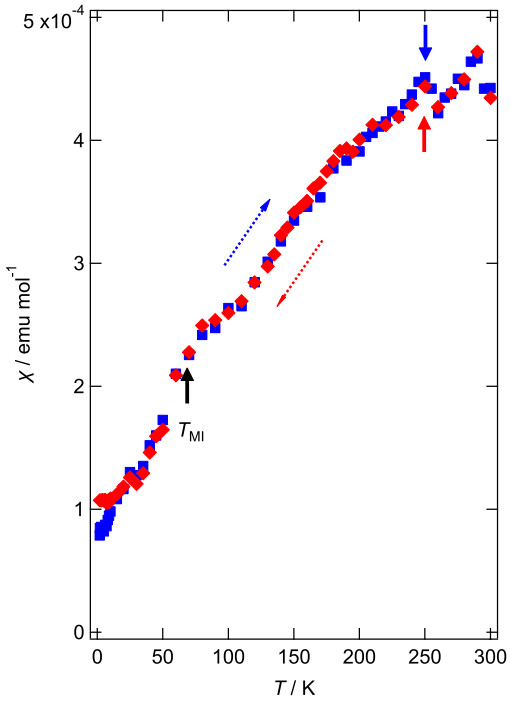

Figure 5. Temperature-dependent magnetic susceptibility of **2** after subtracting 0.084 % of Curie tail.

When the shortest O···O distance ($O\cdots O_{rotation}$) between the anions estimated considering the rotational disorder (Figure 6), Compound **1L** results in 3.079 Å (Figure 7a), whereas Compound **2** leads to an unreasonably short distance of 2.24 Å (Figure 7b) because the anion orientation is also disordered. Accordingly, the rotational disorder is impossible in Compound **2**. The detail is discussed in the Additional structural discussion section in Supporting Information.

Moreover, the S-O bond lengths of $-SO_3^-$ with occupancy of 87 % are almost the same but those with occupancy of 13 % vary. One is much longer than the other two, as shown in

Figure 8 at several temperatures from 100 to 290 K. This suggests that the negative charge on the major sulfonate is equally distributed but the negative charge on the minor sulfonate is almost localized on a single O atom and the other two O atoms are almost neutral (see inset of the schematic diagram in Figure 8). The monoanionic O atom is located further from the rest of the group, which is suitable to reduce the Coulombic repulsion. Therefore, in summary, rotation of the minor sulfonate would increase the interatomic Coulombic repulsion because the monoanionic O atom would be in closer contact with an O atom of the major sulfonate. Thus, the 180° orientational disorder and the non-equally distributed negative charge of the minor sulfonate prevent both sulfonates from rotating.

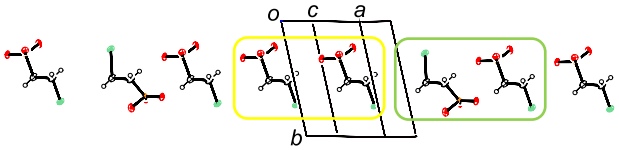

Figure 6. A possible disordered crystal structures of **2** where 13 % of 180° rotated anions exist in the anion chain.

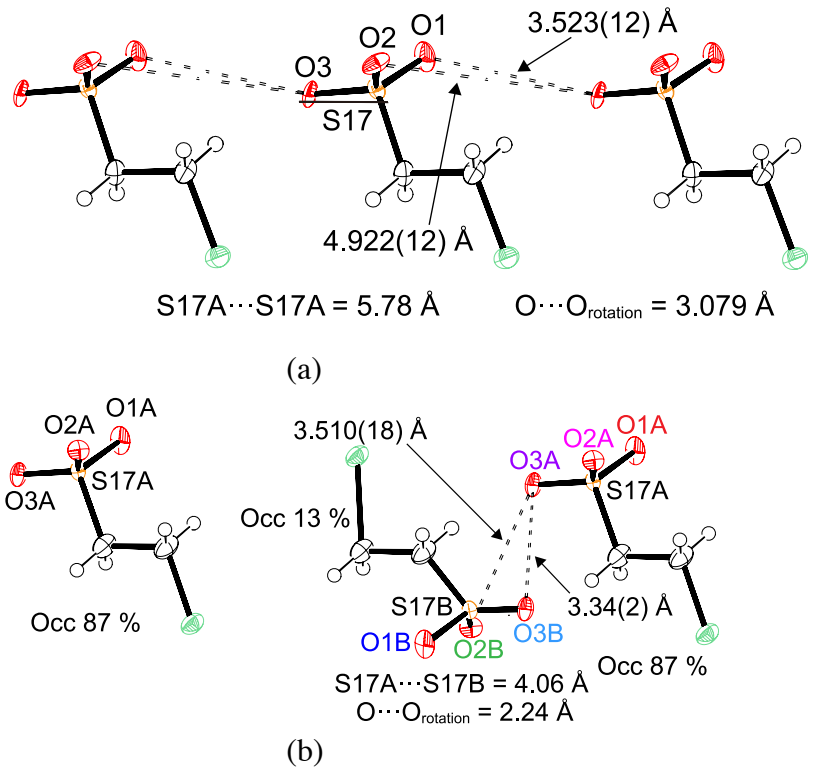

Figure 7. (a) The relation between two neighbour anions of **1**. (b) The relation between the major and minor anions (green rectangle in Figure 6) in the disordered anion chain of **2**, where the occupancies of major and minor anions are 0.87 and 0.13, respectively, at 100 K.

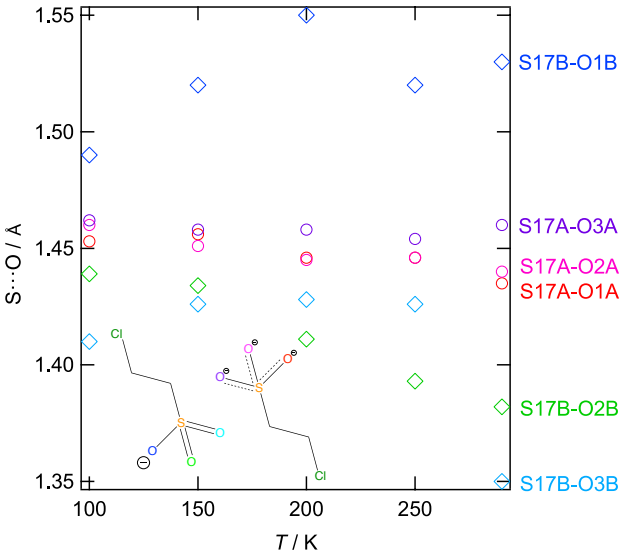

Figure 8. Temperature dependence of S-O bond lengths of the major and minor sulfonates. Inset shows schematic molecular structures of the major (right) and minor (left) molecules.

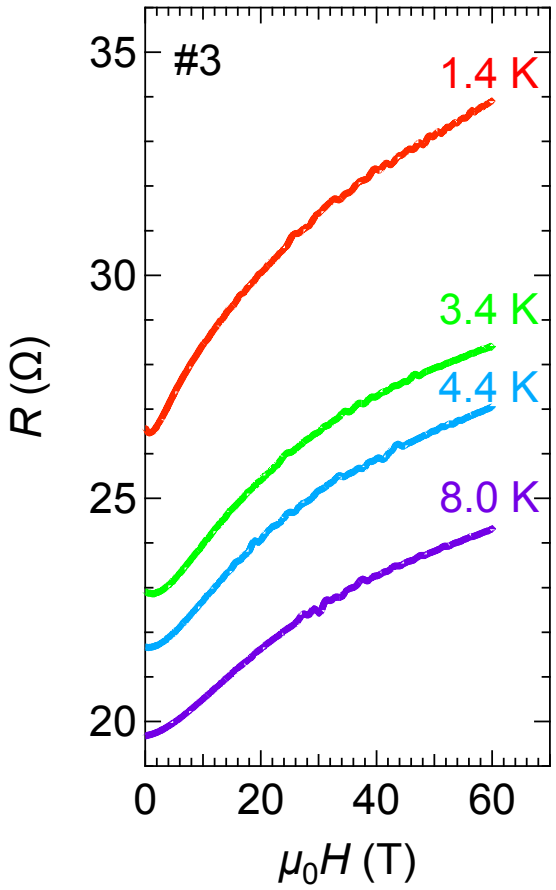

Figure 9. $R(\Omega)$-$\mu_0 H(T)$ plots of the magnetic field dependence of electrical resistivity (MR) of **2**.

Band structure calculations of the A and B layers of **2** were performed,[15] as shown in Figure S3. The results are quite similar to those of **1L**,[11] suggesting that the difference in electronic structures is not the reason for the absence of a structural phase transition.

The magnetic field dependence of electrical resistivity of **2** is shown in Figure 9. **1L** showed a Shubnikov-de Haas (SdH) oscillation since the compound is a semiconductor at the measured temperature but the anion polarity-induced doping provided a small Fermi surface.[11] However, as shown in Figure 9, **2** does not show any SdH oscillations. This could be a consequence of the disorder in each anion chain breaking the periodicity of the crystal and

electronic structures, which is indirect evidence that the structure of the disorder of **2** is like Figure 6 but not Figure S1. Temperature dependence of electrical resistivity of **1** and **2** are shown in Figure S4 up to 200 K.

The Raman spectrum of **2** is shown in Figure S5. At 10.2 K the ν_2 modes split, but by a larger than expected amount, calculated from the estimated charge difference between A and B layers. However, the spectra are also noisy and so this splitting cannot be definitively assigned to the effect of the charge difference. Therefore, the evidence for a charge difference is weak. Although as the temperature is increased, the splitting becomes less clear.

Conclusions

2 does not show any structural phase transition from 300 to at least 100 K, whereas **1** displays a transition. This is despite **2** being isostructural with **1L**. The presence of orientational disorder in the anionic layer of **2** appears to inhibit **2** from showing the phase transition.

Supporting Information

The Supporting Information is available free of charge at https://pubs.acs.org/doi/10.1021/acs.inorgchem.???????.

Additional structural discussion; figure of the crystal structure; figures of band structural calculation; figure of transport properties of **1** and **2**; and Raman spectra (PDF).

AUTHOR INFORMATION

Corresponding Author

Hiroki Akutsu - Department of Chemistry, Graduate School of Science, Osaka University, 1-1, Machikaneyama, Toyonaka, Osaka 560-0043, Japan; https://orcid.org/0000-0002-8350-2246, Email: akutsu@chem.sci.osaka-u.ac.jp.

Author Contributions

The manuscript was written through the contributions of all authors.

Funding Sources

This work was partly supported by Scientific Research C (JP17K05751) from the Japan Society for the Promotion of Science (JSPS).

Notes

The authors declare no competing financial interest.

ACKNOWLEDGMENT

A part of this work was conducted in Institute for Molecular Science, supported by Advanced Research Infrastructure for Materials and Nanotechnology (JPMXP1222MS1032) of the Ministry of Education, Culture, Sports, Science and Technology (MEXT), Japan.

REFERENCES

(1) Mori, T. *Electronic Properties of Organic Conductors*; Springer Japan, 2016.

(2) Akutsu, H.; Yamada, J.; Nakatsuji, S.; Turner, S. S. A novel BEDT-TTF-based purely organic magnetic conductor, α-(BEDT-TTF)$_2$(TEMPO-N(CH$_3$)COCH$_2$SO$_3$) · 3H$_2$O. *Solid State Commun*. **2006**, *140*, 256-260. DOI: 10.1016/j.ssc.2006.07.034.

(3) Akutsu, H.; Yamashita, S.; Yamada, J.; Nakatsuji, S.; Hosokoshi, Y.; Turner, S. S. A Purely Organic Paramagnetic Metal, ϰ-β″-(BEDT-TTF)$_2$(PO-CONHC$_2$H$_4$SO$_3$), Where PO = 2,2,5,5-Tetramethyl-3-pyrrolin-1-oxyl Free Radical. *Chem. Mater*. **2011**, *23*, 762-764, DOI: 10.1021/cm100984z.

(4) Akutsu, H.; Kawamura, A.; Yamada, J.; Nakatsuji, S.; Turner, S. S. Anion polarity-induced dual oxidation states in a dual-layered purely organic paramagnetic charge-transfer salt, (TTF)$_3$(PO-CON(CH$_3$)C$_2$H$_4$SO$_3$)$_2$, where PO = 2,2,5,5-tetramethyl-3-pyrrolin-1-oxyl free radical. *CrystEngComm* **2011**, *13*, 5281-5284. DOI: 10.1039/C1CE05578J.

(5) Akutsu, H.; Ishihara, K.; Yamada, J.; Nakatsuji, S.; Turner, S. S.; Nakazawa, Y. A strongly polarized organic conductor. *CrystEngComm* **2016**, *18*, 8151-8154. DOI: 10.1039/C6CE01865C.

(6) Akutsu, H.; Turner, S. S.; Nakazawa, Y. New Dmit-Based Organic Magnetic Conductors (PO-CONH-C$_2$H$_4$N(CH$_3$)$_3$)[*M*(dmit)$_2$]$_2$ (*M* = Ni, Pd) Including an Organic Cation Derived from a 2,2,5,5-Tetramethyl-3-pyrrolin-1-oxyl (PO) Radical. *Magnetochem*. **2017**, *3*, 11. DOI: 10.3390/magnetochemistry3010011.

(7) Akutsu, H.; Ito, S.; Kadoya, T.; Yamada, J.; Nakatsuji, S.; Turner, S. S.; Nakazawa, Y. A new Ni(dmit)$_2$-based organic magnetic charge-transfer salt, (*m*-PO-CONH-*N*-methylpyridinium)[Ni(dmit)$_2$]·CH$_3$CN, *Inorg. Chim. Acta* **2018**, *482*, 654-658. DOI: 10.1016/j.ica.2018.07.003.

(8) Akutsu, H.; Ishihara, Ito, S.; Nishiyama, F.; K.; Yamada, J.; Nakatsuji, S.; Turner, S. S.; Nakazawa, Y. Anion Polarity-Induced Self-doping in Purely Organic Paramagnetic Conductor, α´-α´-(BEDT-TTF)$_2$(PO-CONH-*m*-$C_6H_4SO_3$)·H_2O where BEDT-TTF is Bis(ethylenedithio)tetrathiafulvalene and PO is 2,2,5,5-Tetramethyl-3-pyrrolin-1-oxyl Free Radical, *Polyhedron* **2017**, *136*, 23-29. DOI: 10.1016/j.poly.2017.02.001.

(9) Akutsu, H.; Kohno, A.; Turner, S. S.; Yamashita, S.; Nakazawa, Y. Different electronic states of isomorphous chiral vs. racemic organic conducting salts, β´´-(BEDT-TTF)$_2$(*S*- and *rac*-PROXYL-CONHCH$_2$SO$_3$), *Mat. Adv.* **2020,** *1*, 3171-3175. DOI: 10.1039/d0ma00694g.

(10) Akutsu, H.; Koyama, Y.; Turner, S. S.; Nakazawa, Y. Structures and Properties of New Organic Molecule-Based Metals, (D)$_2$Br$C_2H_4SO_3$ [D = BEDT-TTF and BETS]. *Magnetochem.* **2021**, *7*, 91. DOI: 10.3390/magnetochemistry7070091.

(11) Akutsu, H.; Uruichi, M.; Imajo, S.; Kindo, K.; Nakazawa, Y.; Turner, S. S. Temperature and pressure induced doping in organic conductors β´´-(BEDT-TTF)$_2$X$C_2H_4SO_3$ (X = Cl and Br). *J. Phys. Chem. C* **2022**, *126*, 16529-16538. DOI: 10.1021/acs.jpcc.2c05126.

(12) Akutsu, H.; Nakazawa, Y.; Turner, S. S. A 2D interactive spin ladder system, δ´-(BEDT-TTF)$_2$Cl$C_2H_4SO_3$·H_2O. *Cryst. Growth Des.* **2022**, *22*, 5143-5147. DOI: 10.1021/acs.cgd.2c00727.

(13) Stewart, J. J. P. Stewart Computational Chemistry, Colorado Springs, CO, USA, http://OpenMOPAC.net. **2016**.

(14) Suda, M.; Kameyama, N.; Ikegaki, A.; Einaga, Y. Reversible Phototuning of the Large Anisotropic Magnetization at the Interface between a Self-Assembled Photochromic Monolayer and Gold. *J. Am. Chem. Soc.* **2009**, *131*, 865-870. DOI: 10.1021/ja808231c.

(15) Mori, T.; Kobayashi, A.; Sasaki, Y.; Kobayashi, H.; Saito, G.; Inokuchi, H. The Intermolecular Interaction of Tetrathiafulvalene and Bis(ethylenedithio)tetrathiafulvalene in Organic Metals. Calculation of Orbital Overlaps and Models of Energy-band Structures. *Bull. Chem. Soc. Jpn.* **1984**, *57*, 627-633. DOI: 10.1246/bcsj.57.627.

(16) We have determined crystal structures of the crystal of 2 at 290, 250, 200, 150 and 100 K, at which we have refined the occupancies of disordered anions, which are 0.846(2)/0.154(2), 0.855(2)/0.145(2), 0.858(2)/0.142(2), 0.862(2)/0.138(2) and 0.873(18)/0.127(18), respectively. In this paper, if not mentioned, we use the observed values at 100 K.

TOC graphics

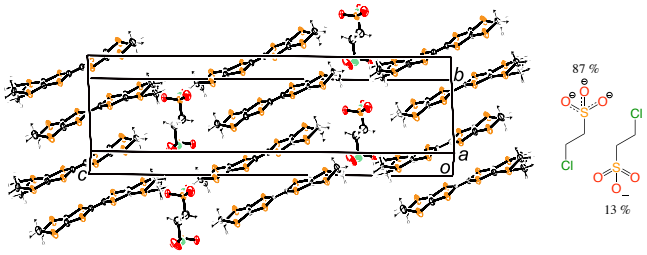

Synopsis

An organic conductor β´´-β´´-(BEDT-TTF)$_2$ClC$_2$H$_4$SO$_3$ (**2**) possessing orientationally disordered anionic layers does not show any phase transitions from 300 to at least 100 K, whereas the low temperature phase (**1L**) of the already reported salt (**1**), whose chemical composition and cell

parameters are the same as **2**, displays an order-disorder transition of rotational motion of -SO_3^-. The presence of orientational disorder in the anionic layer of **2** appears to inhibit **2** from showing the transition.